IMPROVING THE TREATMENT OF SALINE BRINES IN EWASG FOR THE SIMULATION OF HYDROTHERMAL SYSTEMS

Alfredo Battistelli

RISAMB Dept., Saipem SpA
Via Toniolo 1, Fano, 61032, Italy
e-mail: alfredo.battistelli@saipem.com

ABSTRACT

The EWASG EOS module was developed within the frame of the TOUGH2 numerical reservoir simulator for the modeling of hydrothermal systems containing salt and a non-condensable gas (NCG). The code version distributed in 1999 suffered, however, from a few notable limitations: brine correlations are derived from different sources, with the potential risk of limited internal coherence; brine correlations do not properly cover the entire P-T-X space of interest; and NCG effects are evaluated with an approach limited to low partial pressures.

Improvements developed so far to overcome some of the above limitations are described in the present work, with regard to the modeling of saline hydrothermal systems. It must be reiterated that the brine treatment employed by EWASG was subsequently inherited by other EOS modules such as ECO2, ECO2N, EOSM, TMVOC V.2.0, and TMGAS. Described improvements can be easily implemented in other TOUGH2 EOS modules dealing with NaCl solutions.

INTRODUCTION

The EWASG EOS module (Battistelli et al., 1993; Battistelli et al., 1997) was developed within the frame of the TOUGH2 (Pruess, 1991) numerical reservoir simulators, and then distributed by LBNL embedded into TOUGH2 V.2 (Pruess et al., 1999). Since then, EWASG was included within the inverse simulation code iTOUGH2 (Finsterle, 2007) and the parallel code version TOUGH-MP (Zhang et al., 2008). It was also used by LBNL as the starting point for ECO2 (Pruess and Garcia, 2002) and then ECO2N (Pruess, 2005), the latter widely used for the modeling of geological sequestration of supercritical CO_2 in saline aquifers. The correlations for NaCl properties are also used in TMVOC V.2.0 (Battistelli, 2008) for environmental applications, TMGAS (Battistelli and Marcolini, 2009) for GHG sequestration and acid gas mixtures injection, and EOSM (Pruess, 2011) for CO_2 sequestration in saline aquifers under sub- and supercritical conditions.

EWASG is used primarily for modeling hydrothermal systems containing dissolved solids and noncondensable gases. The version distributed in 1999 suffered, however, from some key limitations: brine correlations are derived from different sources, with the potential risk of limited internal coherence. Moreover, brine correlations do not cover properly the entire P-T-X space of interest (T=0-350°C; P=0-1000 bar; XS=0-1). In addition, the effects of NCG are evaluated with an approach limited to low partial pressures of the noncondensable gas.

Since the initial delivery of the code, several improvements have been implemented in an attempt to overcome the above limitations and extend the applicability of EWASG to a wider range of thermodynamic conditions (Battistelli et al., 2009). Some of the main improvements included are described in the present work:

- IAPWS-IF97 correlations for pure water and steam (IAPWS, 1997) and a more recent formulation for water and steam viscosity (IAPWS, 2008).
- An internally consistent H_2O-NaCl EOS package derived from the work of Driesner and Heinrich (2007) and Driesner (2007).
- A more consistent approach of vapor pressure lowering (VPL) and water adsorption, including the dependency of capillary pressure on temperature and salt concentration.

IAPWS-IF97 CORRELATIONS

TOUGH2 V.2 uses the IFC67 correlations (IFC, 1967) for computing vapor pressure, density, and the internal energy of liquid water and steam within the following regions of P-T space:

Region 1: liquid water to 350°C and 1000 bar;

Region 2: steam up to 800°C and 1000 bar;

Region 4: vapor pressure up to the critical point of water.

The IAPWS-IF97 formulation (IAPWS, 1997) is made available within TOUGH2 as summarized in Table 1. The relative subroutines were kindly supplied by Michael O'Sullivan (Croucher and O'Sullivan, 2008). A more recent formulation for the dynamic viscosity of water and steam has been coded (IAPWS, 2008) that computes more accurate viscosity values at high temperatures. The new subroutines are included into the T2F.f module and can be invoked in a TOUGH2 simulation run using a flag from the SELEC block in the input file. Even though the correlations are officially limited to 350°C for liquid water, they can be safely used up to 360°C and, with minor errors, up to 370°C.

Table 1. New subroutines for the properties of liquid water and steam.

Subroutine	Region	Property
COWAT97	1	density and internal energy of liquid water
SUPST97	2	density and internal energy of steam
SAT97	4	saturation pressure
TSAT97	4	saturation temperature
VISH2008	1, 2 & 4	water and steam dynamic viscosity

NEW EOS FOR H_2O-NACL MIXTURES

Driesner and Heinrich (2007) (D&H) revised published data on H_2O-NaCl-phase boundaries up to 1000°C and 5000 bar, and for mixtures ranging from pure water to pure salt compositions. Driesner (2007) presented a comprehensive set of correlations for the computation of phase-mixture properties over the above P-T-X space. D&H computed pure water properties using the IAPS-84 formulation as described by Haar et al. (1984). In implementing the D&H approach into the TOUGH2 framework, the IAPWS-IF97 correlations have been used to evaluate pure water properties in Regions 1, 2, and 4. Thus, the H_2O-NaCl EOS implemented into EWASG is limited to temperatures up 350°C, and with minor errors up to 370°C; pressures up 1000 bar and NaCl concentrations from 0 up to saturation.

D&H used the same molecular weight of water implemented into TOUGH2, 18.015 g/mol, but a slightly different molecular weight for the NaCl: 58.443 g/mol against 58.448 g/mol used in EWASG (Battistelli et al., 1997). Thus, the value of 58.443 g/mol is used with the D&H model. As in EWASG, the D&H reference condition for the brine enthalpy is pure liquid water with zero enthalpy at the triple point of water (0.01°C, P=611.73 Pa). (The main equations are restated below; for the whole set of correlations and related coefficients, I refer the reader to the papers by D&H.)

Brine density

The computation is performed according to Driesner (2007) by determining the temperature T_V*, as a function of pressure and salinity, at which the pure water has the same molar volume V_b of the brine at temperature T (°C), pressure P (bar) and salt molar fraction X_{NaCl}, as expressed by Eq. (1).

$$V_b(T,P,X_{NaCl}) = V_{H2O}(T_V^*,P) \tag{1}$$

All related equations are included into the new subroutine DRIESNER, called by COBRI if the D&H model is selected from the input file. The mass density of the brine is computed from that of pure water using the molecular weights as shown in Eq. (2).

$$\rho_b(T,P,X_{NaCl}) = \rho_{H2O}(T_V^*,P)\frac{PM_b}{PM_{H2O}} \tag{2}$$

where the brine molecular weight PM_b is computed from the mass fraction of salt XS in a straightforward way. Driesner (2007) also suggests corrections of Eq. (1) in specific ranges of P-T-X space, which have been also implemented into the DREISNER subroutine.

In Fig. 1, the brine density calculated as a function of salinity using EWASG, D&H and the BRNGAS correlation of Pritchett (1993), already included in TMVOC V.2.0, TMGAS and EWASG, is compared with the density data tabulated by Pitzer et al. (1984) at 800 bar and

300°C. Then BRNGAS correlation starts to underestimate the density at 200°C, while the D&H model reproduces Pitzer's density well at all temperatures.

Brine enthalpy

Following Driesner (2007), a similar approach is used for the brine enthalpy. The temperature T_H*, as a function of pressure and salinity, is the

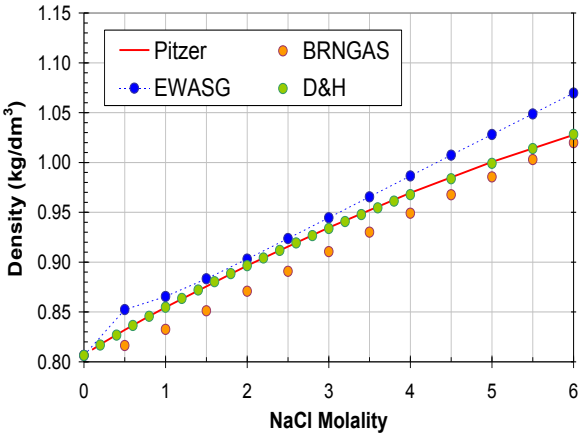

Figure 1. Brine density at 800 bar and 300°C. Comparison among values computed with EWASG, Pritchett (1993) and Driesner (2007) correlations and those published by Pitzer et al. (1984).

temperature at which pure water has the same enthalpy h_b of the brine at temperature T (°C), pressure P (bar), and salt molar fraction XNaCl, as expressed by Eq. (3).

$$h_b(T,P,X_{NaCL}) = h_{H2O}(T_H^*,P) \quad (3)$$

The necessary equations have been coded into subroutine DRIESNER called by COBRI.

Halite density

The density of solid salt (halite) is computed following Driesner (2007) by adding, to the density of halite at zero pressure, a correction proportional to the pressure as shown by:

$$\rho_{halite} = \rho^0_{halite}(T) + l(T)\,P \quad (4)$$

The correlation is included in subroutine DHAL.

Halite solubility

Halite solubility is computed in EWASG as a function of temperature using a correlation due to Potter and quoted by Chou (1987). Dreisner and Heinrich (2007) computed the brine composition at equilibrium with halite as a function of both temperature and pressure, using Eq. (5), where coefficients e_i are functions of pressure P (bar):

$$X^L_{NaCl,sat} = \sum_{i=0}^{5} e_i \left(\frac{T}{T_{hm}}\right)^i \quad (5)$$

T_{hm} is the temperature of halite melting:

$$T_{hm} = T_{triple,NaCl} + a(P - P_{triple,NaCl}) \quad (6)$$

The solubility dependence from pressure becomes remarkable only for temperatures higher than about 450°C and for very high pressures, as shown by Driesner (2007). Within our field of interest, temperatures lower than 400°C, the solubility dependence of pressure up to 1000 bar is negligible. Thus, the above D&H correlation was not included in EWASG, to avoid an increase in computation effort for a negligible increase in accuracy.

Halite solubility at 1 bar up to 100°C and then at the brine-saturation pressure for higher temperatures has been computed using Eq. (5). Computed values are compared in Fig. 2 to the solubility calculated within EWASG and to the values computed according to Palliser and McKibbin (1998) (P&McK).

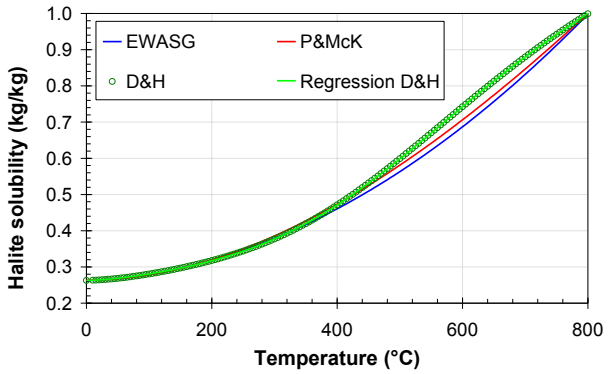

Figure 2. Halite solubility computed using EWASG, Palliser and McKibbin (1998) and Driesner and Heinrich (2007).

The standard EWASG correlation reproduces the D&H values up to 350°C with an error lower than 1%, while the P&McK's correlation has a higher error. Conversely, at high temperature, P&McK's correlation performs slightly better and is closer to D&H values. D&H solubility values have been regressed as a function of

temperature, using a polynomial expression included in subroutine HALITE.

Halite enthalpy

Halite enthalpy in EWASG is computed, as a function of temperature only, by integrating the specific heat given by Silvester and Pitzer (1976). The chosen reference state for halite enthalpy is that of the triple point of water (T=0.01°C, P=611.73 Pa) at which halite enthalpy is set to zero. Driesner (2007) supplies a correlation for the specific heat of halite as a function of both temperature and pressure, as shown by Eq. (7):

$$c_{P,halite} = r_0 + 2r_1(T - T_{triple,NaCl}) + 3r_2(T - T_{triple,NaCl})^2 + r_3 P + r_4 P^2 \qquad (7)$$

Coefficients r_0, r_1, and r_2 are constants, while r_3 and r_4 are polynomials of third degree with respect to temperature. Integrating the specific heat, Driesner considers the triple point of halite as the reference state for halite enthalpy, in order to be consistent with the reference assumed for the enthalpy of pure water. For comparison purposes, the halite enthalpy as been computed as a function of temperature, assuming zero enthalpy at the triple point of water, and at pressure of 1 bar, integrating the specific heat of Eq. (7); using the standard EWASG code; and by integrating the specific heat given by Pitzer et al. (1984). Computed enthalpy is shown in Fig. 3.

The plot shows good agreement as far as the reproduction of enthalpy at low pressure is concerned among the three approaches.

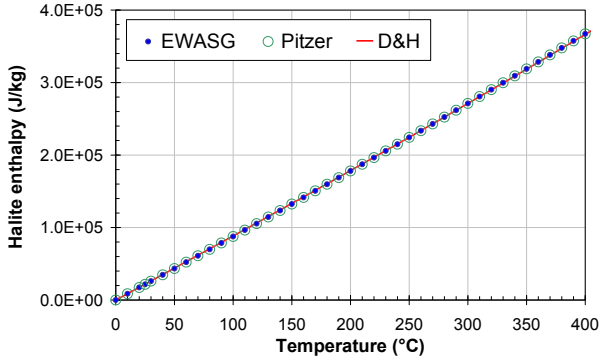

Figure 3. Halite enthalpy computed using EWASG and by integrating the specific heat given by Pitzer et al. (1984) and by Driesner (2007) assuming zero enthalpy at 0.01°C.

The effect of pressure is the increment of halite enthalpy by an amount, proportional to the pressure, which is almost constant in the temperature range of interest for EWASG (T< 400°C). The enthalpy at 1 bar has been computed with a 3rd degree polynomial shown in Eq. (8), while the pressure correction is made using Eq. (9). The error with respect to the enthalpy computed using the SOWAT code (Driesner, 2007) at 400°C and 500 bar is lower than 0.2% and is considered satisfactory for the purposes of EWASG improvement.

$$h_{halite}(T,1bar) = 8.8101E-5\,T^3 + 6.4139E-2\,T^2 + 8.7664E2\,T - 5.6125E5 \qquad (8)$$

$$h_{halite}(T,P) = h_{halite}(T,1bar) + 44.14(P - 1bar) \qquad (9)$$

The new correlation has been included in function HHAL to substitute for the old correlation. In fact, D&H enthalpy reference conditions are different from those assumed in the old EWASG; they are congruent with the computation of water and brine enthalpy, but this was not the case for the old EWASG. Because of that, the calculation of heat effects during precipitation or dissolution of halite are affected by an error in the old EWASG code. This error is insignificant for most applications, but can yield noticeable effects when localized precipitation/dissolution determine large changes in solid salt saturation.

Brine vapor pressure

In EWASG the vapor pressure of sodium chloride brines is computed as a function of temperature and salinity, using a correlation by Haas (1976) calibrated over experimental data covering a temperature range from –11 to 300°C. Driesner and Heinrich (2007) present a new correlation covering a wider field of temperatures and salinities although with a much more complex approach, as shown by Eq. (10).

$$X_{NaCl}^{VL,liq} = X_{crit} + g_0\sqrt{P_{crit} - P} + g_1(P_{crit} - P) + g_2(P_{crit} - P)^2 \qquad (10)$$

In fact, Eq. (10) gives the composition of saturated liquid brine at the vapor pressure P, and as a function of brine critical pressure P_{crit} and composition X_{crit}. Terms g_1 and g_2 are functions of temperature, while g_0 is not explicitly given by D&H and needs to be evaluated with the

constraint that Eq. (10) should deliver the NaCl concentration on the equilibrium surface V+L+H at temperatures lower than the triple point of NaCl (800.7°C).

The SOWAT code has been used to compute the composition of saturated brine as a function of pressure along isotherms from 150 to 350°C. Fig. 4 shows the comparison among these values and those computed using the Haas (1976) correlation implemented in EWASG. Fig. 4 shows negligible differences up to 250°C, which increase at higher temperatures and for salinities greater than 5% by mass. Differences are noticeable at 350°C, because Haas's correlation was calibrated using experimental data at T lower than 300°C.

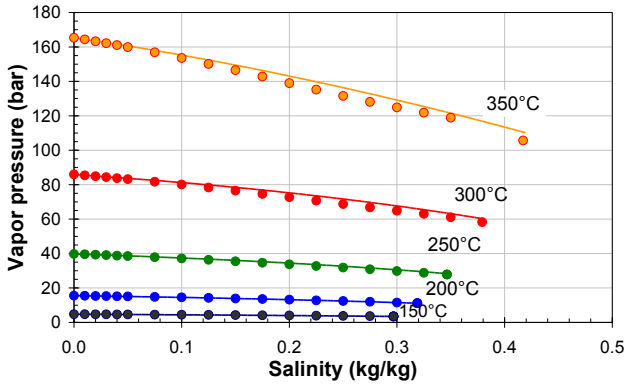

Figure 4. Comparison of saturated brine pressure as function of salinity at different temperatures computed using Haas (1976) (circles) and Driesner and Heinrich (2007) (lines) correlations.

Due to the complexity of the D&H correlation, which would also require an iterative approach, Eq. (10) has not yet been implemented within EWASG. The planned alternative approach is as follows:

- Use the SOWAT code to compute salinity-vapor pressure values for isotherms going from 0.01°C to 400°C;
- Use a new calibration of the coefficients present in the Haas (1976) correlation to reproduce the brine vapor pressure computed by SOWAT.

SUCTION PRESSURE EFFECTS

To model fractured geothermal reservoirs with low matrix permeability and high capillary pressure, it is necessary to account for suction pressure effects. These have already been studied by several authors, who focused either on the processes at low water saturation involving vapor pressure lowering (VPL) effects (O'Sullivan and Pruess, 1995; Battistelli et al., 1998), or on water adsorption processes in vapor-dominated reservoirs (Nghiem and Ramey, 1991; Sta. Maria and Pingol, 1996). VPL has been included in EWASG by using the Kelvin's equation as given by Eq. (11). The vapor partial pressure under two-phase conditions is obtained by multiplying the saturation pressure times the VPL factor given by Eq. 11.

$$f_{VPL} = \exp\left[\frac{W^{H2O} P_{cap}(S_L)}{\rho_L(P_L, T, X_L^{NaCl}) R(T + 273.15)}\right] \quad (11)$$

Phase equilibrium is solved assuming the additivity of partial pressures of water vapor and of the NCG. In EWASG, the aqueous-phase density in Kelvin's equation is computed using the aqueous-phase pressure.

Modeling of vapor adsorption

VPL is described using distinct approaches, even though they are different aspects of the same process: the vapor adsorption on the rock surface, and the capillary condensation of aqueous phase. In both cases, the aqueous phase is present under metastable conditions at a pressure lower than the saturation pressure for local temperature. The presence of two-phase conditions instead of single steam, in a vapor-dominated reservoir, has strong implications for the amount of fluid initially stored in the reservoir. Even small saturations of liquid water can contribute substantially to the mass of fluid stored in the unit reservoir volume.

Adsorption and capillary condensation have usually been described with different modeling approaches. In addition to Kelvin's equation used in the TOUGH2 simulator (Pruess and O'Sullivan, 1992; Pruess et al., 1999), the vapor adsorption is described with adsorption isotherms, as generated by Stanford University researchers, who made prolonged experimental studies on rock samples collected at The Geysers and Larderello steam-dominated geothermal fields. The adsorption isotherms are described with several formulations, among which the classical one is that due to Langmuir (Nghiem

and Ramey, 1991), as expressed by Eq. 12. X^W is the mass fraction of water with respect to rock mass, and A and B are experimental coefficients:

$$X^W = \frac{A\, f_{VPL}}{1 + B\, f_{VPL}} \tag{12}$$

It is useful to model (with a unique formulation) both adsorption and capillary condensation within a reservoir simulator. Sta Maria and Pingol (1996) observed that adsorption isotherms are generally able to describe experimental results for values of VPL coefficients lower than 0.9, while Kelvin's equation has difficulty at low water saturation values, when the capillary pressure becomes extremely high. The adsorption isotherm establishes a relationship between the mass of absorbed water and the VPL coefficient. Assuming that the density of adsorbed water can be estimated with conventional correlations at saturated conditions, from rock porosity and grain density, it is possible to convert the adsorbed mass in an equivalent liquid saturation, assuming also that adsorbed water on grain surfaces occupies a fraction of pore volume. The equivalent liquid saturation is given by Eq. 13 (Sta. Maria and Pingol, 1996):

$$S_{Aq} = \frac{1-\varphi}{\varphi}\frac{\rho_R}{\rho_{Aq}} X^W \tag{13}$$

This saturation can be used to determine the capillary-pressure value, which reproduces the experimental VPL coefficients computed with the Kelvin equation. Adsorption and capillary pressure data can then be combined for a regression on a unique capillary-pressure curve.

Dependency of capillary pressure on surface tension

Both adsorption and capillary-condensation processes are function of temperature. The capillary pressure depends in fact on the surface tension between the two phases at equilibrium. For steamwater two-phase conditions, the surface tension decreases with temperature, to vanish at the water critical temperature. The capillary-pressure values obtained for a given pair of fluids can be normalized using the J-Leverett function (Leverett, 1941):

$$J(S_{Aq}) = \frac{P_c}{\sigma \cos\theta}\sqrt{\frac{k}{\varphi}} \tag{14}$$

where σ is the surface tension (N/m) (IFT), θ is the contact angle, k the absolute permeability (m^2) and φ is rock porosity. Once the J-Leverett function is obtained with a regression on experimental data for a specific rock formation, the capillary pressure can be computed as a function of petro-physical and fluid properties, as follows:

$$P_c = J(S_W)\,\sigma \cos\theta \sqrt{\frac{\varphi}{k}} \tag{15}$$

IFT is a function of fluid phases at equilibrium, of their composition and local temperature. The J-Leverett function is customarily used to evaluate the capillary pressure at reservoir conditions from laboratory measurements performed at different conditions and with different fluid phases. The temperature affects both IFT and the contact angle, the latter changing also with rock type. Assuming the contact angle changes marginally with temperature, the capillary pressure at reservoir conditions is given by Eq. 16:

$$P_{c,res}(T) = P_{c,lab}(T_{ref})\frac{\sigma(T,X,Y)}{\sigma_{ref}(T_{ref},X,Y)} \tag{16}$$

X and Y represent the composition of aqueous and gaseous phases, respectively. In hydrothermal systems, the gaseous phase contains mainly water vapor and a mixture of NCG, among which CO_2 usually predominates. In the aqueous phase, sodium chloride is generally the predominant dissolved solid. The pure-water IFT is computed in TOUGH2 using subroutine SIGMA (module T2F.f), based on the IAPS (1976) formulation. It differs from the more recent IAPWS (1994) release only in its different definition for the critical point of water, 647.096 K instead of 647.15 K.

The water IFT declines rapidly at increasing temperatures, from 72.74E-3 N/m at 20°C to 58.92E-3, 37.68E-3, 14.37E-3, and 3.67E-3 at 100, 200, 300 and 350°C, respectively. The capillary pressure should then become increasingly less important at reservoir temperatures greater than 300°C, common in the deep zones of many geothermal fields. On the other hand, the presence of salt increases the brine critical temperature substantially. For instance, NaCl mass fractions of 3 and 5%, found in some geothermal fields, increase the critical temperature to 403 and 493°C, respectively.
Thus, brine at 300°C has IFT greater than that of pure water at the same temperature, as it is farther than pure water from its critical temperature. For

instance, Ozdemir et al. (2009) reports experimental data indicating a consistent increment of brine IFT with salt content. Assuming the corresponding state principle is applicable to the IFT, then the IFT of brine at a given NaCl concentration is equal to that of pure water at the same reduced temperature.

Fig. 5 shows the critical temperature of brine as a function of NaCl mass fraction computed using the old EWASG correlation, and P&McK and D&H values. Up to a NaCl fraction of 0.3, the critical temperature is comparable. D&H supplied the relationships between salinity and critical temperature up to 1000°C. Thus, a regression on values given by P&McK has been included in EWASG. Fig. 6 shows the computed brine surface tension as function of temperature for salt mass fractions of 5, 10, 20, and 25% in NaCl.

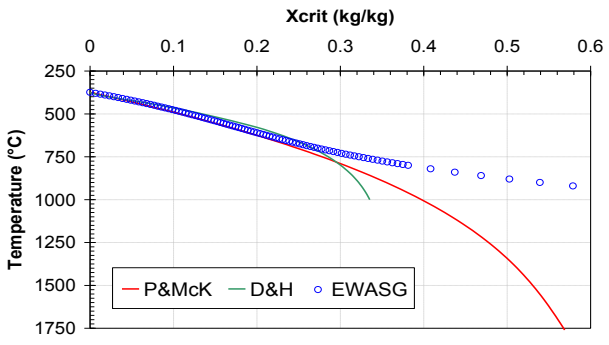

Figure 5. NaCl solubility at critical conditions computed using EWASG, P&McK and D&H.

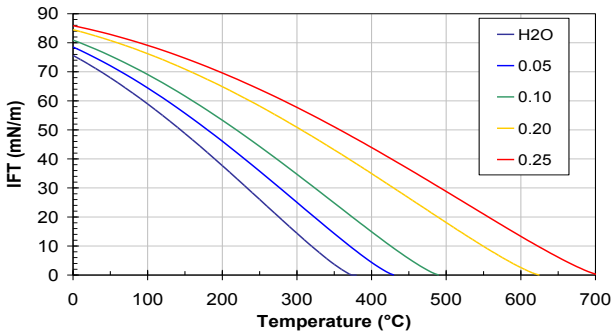

Figure 6. Surface tension of water and NaCl brines as function of temperature assuming the corresponding state principle is applicable.

The computation of capillary pressure in TOUGH2 has been modified, including its dependency on temperature through the brine IFT. The option is invoked giving the reference surface tension (in N/m) to parameter CP(7,nmat) in the ROCKS block of input file. The option is available for the van Genuchten (ICP=7), and Parker (ICP=8) models for water-gas two-phase conditions.

CONCLUSIONS

EWASG allows the modeling of ternary mixtures of water, NaCl, and a NCG within TOUGH2 V.2.0. While developed primarily for hydrothermal systems, the brine correlations have been extensively used in other EOS modules (such as ECO2N, EOSM, TMVOC V.2 and TMGAS) for environmental applications, GHG, and acid gas geological storage. The description of water-NaCl mixtures in EWASG has been improved by implementing correlations recently developed by Driesner and Heinrick (2007) and Driesner (2007). They were able to describe the thermodynamics and calculate phase properties for temperatures from 0 to 1000°C, pressures from 1 to 5000 bar, and NaCl mass fractions from 0 to 1. Pure water properties within EWASG are now computed using the IAPWS-IF97 (1997) and IAPWS (2008) correlations up to 350°C. (They can be used up to 370°C with minor errors.) D&H correlations for brine density and enthalpy are included in a new subroutine DRIESNER, while new correlations for halite density, enthalpy, and solubility have been included in the old EWASG subroutines. The composition of brine at critical conditions is computed using the correlation from Palliser and McKibbin (1998) in closed form.

An approach to describe VPL effects due to both water adsorption and capillary condensation using Kelvin's equation is proposed within TOUGH2, following St. Maria and Pingol (1996). Temperature and salinity effects on capillary pressure at high temperatures are accounted for including IFT effects, following the J-Leverett (1941) normalization.

ACKNOWLEDGMENTS

The management of Saipem SpA is acknowledged for the permission to publish the present work. Thanks are due to Michael O'Sullivan and Adrian Croucher, who kindly supplied the routines for the IAPWS-IF97 correlations.

REFERENCES

Battistelli A., C. Calore, and K. Pruess, *A fluid property module for the TOUGH2 simulator for saline brines with non-condensible gas*. Proc. 18th Work. Geoth. Res. Eng., Stanford Un., CA, 249-259, 1993.

Battistelli A., C. Calore, and K. Pruess K., The simulator TOUGH2/EWASG for modelling geothermal reservoirs with brines and a non-condensible gas. *Geothermics*, 26(4), 437-464, 1997.

Battistelli A., Modeling multiphase organic spills in coastal sites with TMVOC V.2.0. *Vadose Zone Journal*, 7, 316-324, 2008.

Battistelli A., M. Carpita, C. Geloni, and M. Marcolini, *New TOUGH2 EOS modules for the simulation of geothermal reservoirs containing saline brines and non-condensable gases*. GeoTherm Expo, Sept. 23-25, 2009, Ferrara, Italy, 2009.

Croucher A.E., and M.J. O'Sullivan, Application of the computer code TOUGH2 to the simulation of supercritical conditions in geothermal systems. *Geothermics*, 37, 622–634, 2008.

Driesner T., and C.H. Heinrich, The system H_2O–NaCl. Part I: Correlation formulae for phase relations in temperature–pressure–composition space from 0 to 1000°C, 0 to 5000 bar, and 0 to 1 XNaCl. *Geoch. Cosm. Acta*, 71, 4880–4901, 2007.

Driesner T., The system H_2O–NaCl. Part II: Correlations for molar volume, enthalpy, and isobaric heat capacity from 0 to 1000°C, 1 to 5000 bar, and 0 to 1 XNaCl. *Geoc. Cosm. Acta*, 71, 4902–4919, 2007.

Haar L., J.S. Gallagher, and G.S. Kell, *NBS/NRC Steam Tables*. Hemisphere Publ. Corp., 1984.

Haas Jr, J. L. (1976) Physical properties of the coexisting phases and thermochemical properties of the H2O component in boiling NaCI solutions. USGS Bulletin 1421-A.

International Association for the Properties of Water and Steam, *Release on the IAPWS Formulation 2008 for the Viscosity of Ordinary Water Substance*. Berlin, Germany, 2008.

International Association for the Properties of Water and Steam, *Release on the IAPWS Industrial Formulation 1997 for the Thermodynamic Properties of Water and Steam*. Erlangen, Germany, 1997.

International Association for the Properties of Water and Steam,. *Release on Surface Tension of Ordinary Water Substance*, 1994.

International Association for the Properties of Steam, *Release on Surface Tension of water substance*. NBS, Washington, USA, 1976.

International Formulation Committee, *A Formulation of the Thermodynamic Properties of Ordinary Water Substance*, IFC Secretariat, Düsseldorf, Germany, 1967.

Leverett M.C., Capillary Behavior in Porous Solids. *Trans. Soc. Pet. Eng. AIME*, 142, 152-169, 1941.

Ozdemir O., S.I. Karakashev, A.V. Nguyen, and J. Miller, Adsorption and surface tension analysis of concentrated alkali halide brine solutions. *Minerals Eng.* 22(3), 263-271, 2009.

Palliser C., and R. McKibbin, A model for deep geothermal brines. I. T–p–X state–space description. *Transp. Por. Med.*, 33, 65–80, 1998.

Pitzer K.S., Peiper J.C., and Busey R.H. Thermodynamic properties of aqueous sodium chlorides solutions. *J. Phys. Chem. Ref. Data*, 13(1), 1-102, 1984.

Pritchett J. W. *STAR User's manual. Appendix F.1 - The "BRNGAS" equation-of-state*. S-Cubed Report SSS-TR-89-10242, revision A., 1993.

Pruess K., *TOUGH2 A general-purpose numerical simulator for multi-phase fluid and heat flow*. Report LBL-29400, Lawrence Berkeley National Laboratory, Berkeley, Calif., 1991.

Pruess K., C. Oldenburg, and G. Moridis, *TOUGH2 User's Guide, Version 2.0*. Report LBNL-43134. Lawrence Berkeley National Laboratory, Berkeley, Calif., 1999.

Pruess K., and M. O'Sullivan M., *Effects of capillarity and vapor adsorption in the depletion of vapor-dominated geothermal reservoirs*. Proc. 17th Work. Geoth. Res. Eng., Stanford, USA, 165-174, 1992.

Pruess K., and J. Garcia (2002). Multiphase flow dynamics during CO_2 disposal into saline aquifers, *Env. Geology*, 42, 282-295.

Pruess, K., ECO2N : *A TOUGH2 Fluid Property Module Mixtures of Water, NaCl and CO_2*. LBNL Report 57952, Lawrence Berkeley National Laboratory, Berkeley, Calif., 2005.

Silvester L.F., and K.S. Pitzer, *Thermodynamics of geothermal brines I. Thermodynamic properties of vapor-saturated NaCl (aq) solutions from 0-300°C.* Report LBL-4456, Lawrence Berkeley National Laboratory, Berkeley, Calif., 1976.

Sta. Maria R., and A.S. Pingol, *Simulating the effects of adsorption and capillary forces in geothermal reservoirs*. Proc. 21st Work. Geoth. Reservoir Eng., Stanford, CA, SGP-TR-151, 165-173, 1996.

van Genuchten, M.Th., A Closed-Form Equation for Predicting the Hydraulic Conductivity of Unsaturated Soils. *Soil Sci. Soc. Am. J.*, 44, 892 – 898, 1980.

Zhang K., Wu Yu-Shu, and K. Pruess, *User's Guide for TOUGH2-MP - A Massively Parallel Version of the TOUGH2 Code*. Report LBNL-315E, Lawrence Berkeley National Laboratory, Berkeley, Calif., 2008.